Frequency Dependent Noise Temperature of the Lattice Cooled Hot-Electron Terahertz Mixer

A.D.Semenov[a], H.-W. Hübers[b], J.Schubert[b], G.N. Gol'tsman[a], A.I. Elantiev[a], B.M. Voronov[b], and E.M. Gershenzon[a]

[a] Physical Department, State Pedagogical University of Moscow, 119891 Moscow, Russia
[b] DLR Institute of Space Sensor Technology and Planetary Exploration, 12489 Berlin, Germany

ABSTRACT

We present the measurements and the theoretical model on the frequency dependent noise temperature of a lattice cooled hot electron bolometer (HEB) mixer in the terahertz frequency range. The experimentally observed increase of the noise temperature with frequency is a cumulative effect of the non-uniform distribution of the high frequency current in the bolometer and the charge imbalance, which occurs near the edges of the normal domain and contacts with normal metal. In addition, we present experimental results which show that the noise temperature of a HEB mixer can be reduced by about 30% due to a Parylene antireflection coating on the Silicon hyperhemispheric lens.

I. INTRODUCTION

Heterodyne spectroscopy in the frequency range from 1 THz to 6 THz yields important information on astronomical objects as well as on the chemical composition of the earth's atmosphere. Some prominent examples are the CII fine structure line at 1.6 THz and the OI fine structure line at 4.75 THz, which are major coolant lines of the interstellar medium. The OH rotational transitions at 2.5 THz and 3.5 THz allow determination of the OH volume mixing ratio in the stratosphere and provide important information on the catalytic cycles, which are responsible for the destruction of stratospheric ozone [1,2]. Superconducting hot-electron bolometer (HEB) mixers are presently the most promising candidates for quantum limited terahertz heterodyne mixers at frequencies above 1.2 THz. In a sufficiently small device only electrons are heated by the incoming radiation providing the response time of the order of the electron-phonon interaction time. This results in a small noise temperature as well as in intermediate frequencies of several GHz. Another consequence of electron heating only is the small power of the local oscillator, which is required for optimal operation of the HEB mixer.

In this article we report noise temperature measurements performed with the same phonon-cooled NbN HEB mixer in the frequency range from 0.7 THz to 5.2 THz and develop a model that describes the frequency dependence of the mixer performance.

In addition we present results of an experimental investigation of Parylene as an antireflection coating for Si at THz frequencies.

II. MIXER DESIGN AND EXPERIMENTAL DETAILS

The lattice-cooled HEB mixer was manufactured from a thin superconducting NbN film. The film with the nominal thickness 3.5 nm was deposited by dc reactive magnetron sputtering on a 350 μm thick high resistivity (>10 kΩ cm) Si substrate. The details of the process are described elsewhere [3,4]. After deposition films usually had a room temperature square resistance of ≈ 500 Ω that increased to ≈ 660 Ω at 20 K and dropped abruptly to almost zero (residual resistance less than 1 Ω) at the transition temperature close to 10 K. The processing during the device fabrication leads to degradation of superconductivity and the square resistance at room temperature increases up to ≈ 700 Ω (≈ 940 Ω at 20 K) while the transition temperature decreases to a value slightly above 9 K and the transition width increases to ≈ 0.5 K. The bolometer was defined by means of electron beam lithography and represented a 1.7 μm wide and 0.2 μm long bridge connecting the inner terminals of a planar feed antenna. The complementary logarithmic-spiral planar antenna was lithographed from a thermally evaporated gold film (for details see Ref. 4). According to an estimate [5], the complementary spiral antenna should have an impedance of about 75 Ω when suspended in free space. We expect $\varepsilon^{1/2}$ times smaller value for our antenna since it is supported by the dielectric substrate with the dielectric constant ε and the thickness much larger than the wavelength. The substrate with the HEB was glued onto the flat side of an extended hemispherical lens from pure silicon.

The mixer performance was investigated at seven different frequencies ranging from 0.7 THz up to 5.2 THz. Experimental setup, which we used for noise temperature measurements, has been described elsewhere [6]. Briefly, an optically pumped far-infrared gas laser served as local oscillator (LO). Signal radiation from the Eccosorb black body was superimposed on the LO radiation by a mylar 6-μm thick beam splitter. The approximately half-meter long optical path from the black body to the cryostat window was not evacuated. The intermediate frequency (IF) circuit inside the cryostat comprised an isolator associated with a bias tee and a low noise (6 K noise temperature) amplifier. The IF signal was recorded after additional amplification in the 75 MHz bandwidth centered at 1.5 GHz.

III. NOISE TEMPERATURE

Noise temperatures reported in this paper are typical for our devices. The frequency dependence was usually measured with the same device once mounted in the holder. Here we report data obtained with the 6-mm lens without antireflection coating. In Fig. 1 the DSB receiver noise temperature is shown as a function of the LO frequency

between 0.7 THz and 5.2 THz. Also shown is the DSB receiver noise temperature corrected for optical losses.. In this case the increase of the noise temperature with frequency follows closely the 10 $h\nu/k_B$ level. For the estimation of the lower cut-off frequency of our log-spiral antenna we use the criterion [5] $\lambda^*/2 \leq C$ where C is the maximal diameter of the spiral structure and λ^* is the wavelength in the substrate. For our design with C = 130 µm this yields a wavelength in free space of 884 µm (0.34 THz). The wavelength corresponding to the upper cut-off frequency of the antenna is about 10 times the inner radius at which the actual shape deviates from the ideal spiral [7]. In our case this is 1.3 µm yielding the lower limit 44 µm (6.8 THz) for the wavelength in free space. We, therefore, believe that besides conductivity losses in the gold itself the antenna does not contribute any frequency dependence to the noise temperature. For an analysis of the optical losses and the antenna pattern see Ref. [6,8].

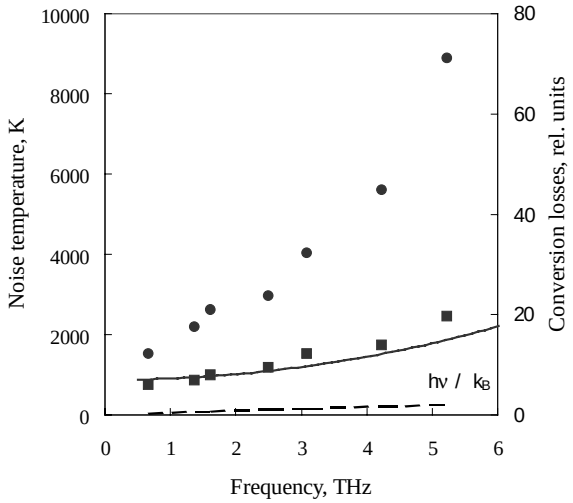

Fig. 1: DSB system noise temperature measured (circles) and corrected (squares) for losses in the optical elements. The dashed line represents the quantum limited noise temperature $h\nu/k_B$. The solid line shows the calculated conversion losses. The scale of the right axis was adjusted in order to match calculated conversion losses and corrected noise temperature.

IV. ANTIREFLECTION COATING

The main contribution to the optical losses originates from the Silicon lens. The uncoated lens has a reflection loss of about 1.5 dB. Therefore an antireflection coating can significantly reduce the receiver noise temperature. Parylene is a good candidate as an antireflection coating. It is a polymer with a refractive index of about 1.62 and therefore matches closely the required value for a single antireflection layer on silicon, which is $n_{Si}^{1/2} \approx 1.84$. Beside this it has a high thermal stability and is chemically inert with low water absorption. Parylene is deposited from the gas phase. This results in films of uniform thickness and high conformity. Parylene exists in different forms. In this study Parylene C was investigated.

Two plane-parallel samples from high resistivity Silicon (> 5 kΩ cm) with a thickness of 5 mm were prepared. One of the samples was coated on one side with a Parylene layer of 18.5 µm thickness while the other remained uncoated. The transmittance of both samples was measured in a Fourier-transform spectrometer in the wavelength range between 100 µm and 320 µm. The results are shown in Fig. 2. The lowest curve displays the transmittance of the uncoated Silicon sample and the curve in the middle displays the transmittance of the coated sample. While the uncoated sample has a transmission between 50% and 53% the coated sample has a peak transmittance of 64% at 130 µm which decreases to 59% and 55% at 100µm and 320 µm, respectively. From these data the transmittance of the coated Silicon surface which is relevant for the quasioptical HEB mixer was calculated assuming multiple reflections inside the Silicon and an absorption coefficient of 0.05 cm^{-1} [9]. The result is presented in the uppermost curve of Fig. 2. A transmittance of 93% at 130 µm is achieved. It stays above 90% between 115 µm and 165 µm. This is sufficient for most practical receiver applications. The solid line in Fig. 2 represents the calculated transmission of a single layer of Parylene on a Silicon substrate.

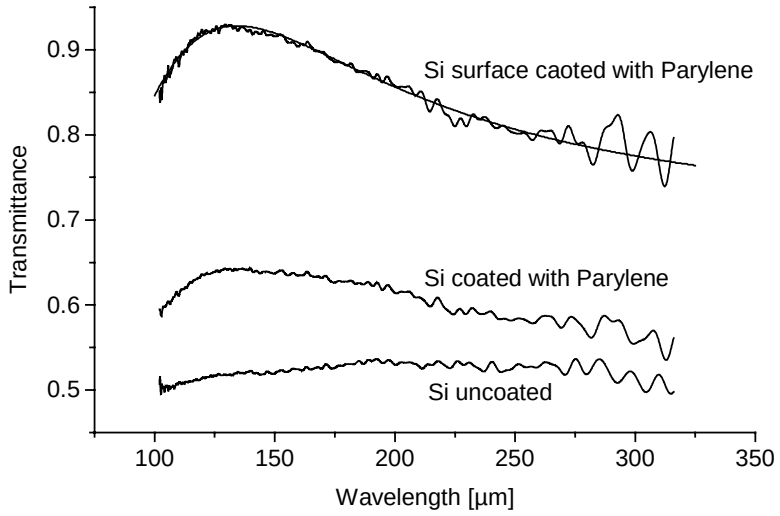

Fig. 2: Transmittance of Silicon with and without a coating of Parylene C.

The thickness of the Parylene layer and its absorption coefficient were chosen to give the best match between the measured and the calculated curve. From this we derive a layer thickness of 20 µm and an absorption coefficient of 25 cm^{-1} for Parylene C. Both are independent of the frequency in the considered range. The thickness as derived from the optical data is slightly higher than measured with a profiler which yielded 18.5 µm. This difference is well in the error limit of both methods. The absorption coefficient is significantly lower than the previously reported one of 75 cm^{-1} [10]. However, all measurements are indirect, i.e. the absorption coefficient is derived from transmittance measurements of a sample coated by Parylene and not by a direct transmission measurement of Parylene itself. In addition the quality of the film may differ and contribute to different absorption coefficients.

The improvement of the noise temperature due to a lens coated with Parylene C was investigated for two HEB mixers. Two lenses each with a diameter of 6 mm were made from the same silicon crystal. One of the lenses was coated with an 18.5 µm thick Parylene C layer.

For both HEB mixers the noise temperature was measured at four different frequencies between 0.7 THz and 2.5 THz by using the coated lens as well as the uncoated lens. In Table 1 the results are shown. A significant improvement of about 30% was achieved at 2.5 THz. This improvement decreases towards the smaller frequencies as it is expected because the thickness of the Parylene layer corresponds to about a quarter wavelength at 2.5 THz. Fig. 3 illustrates the relative improvement, i.e. the difference in noise temperature divided by the noise temperature measured with the uncoated lens. Also shown is the relative improvement as it is expected from the transmittance measurements described above. In this case, the relative improvement is the difference in transmittance between the coated and the uncoated flat Silicon sample divided by the transmittance of the uncoated sample

Freq. [THz]	Device A, T_{rec} [K]		Device B, T_{rec} [K]	
	no AR coating	Parylene coating	no AR coating	Parylene coating
0.693	2200	2100	5300	5300
1.397	2700	2300	7600	5500
1.627	2800	2200	7500	6200
2.523	3900	2500	9400	6500

Table 1: DSB receiver noise temperature for two HEB mixers. Both were measured with a Silicon lens with and without a Parylene antireflection coating.

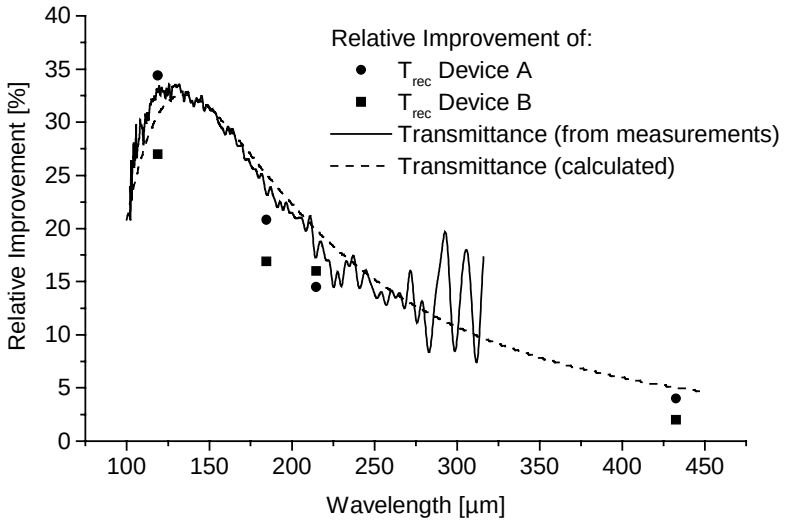

Fig. 3: Relative improvement of noise temperature and transmittance due to coating with Parylene C.

V. FREQUENCY DEPENDENCE OF THE MIXER PERFORMANCE

We discuss now features, which can not be understood in terms of the traditional hot-electron model. This model suggests that the mixers under optimal operation may be driven into either quasi-homogeneous [11] or non-uniform resistive state [12,13]. In both cases, though, the energy of the quantum corresponding to the LO frequency is supposed to be large

compared to the actual magnitude of the energy gap. Consequently, it is further supposed that absorption of radiation in the mixer is spatially uniform while the Joule heating due to bias occurs only in those parts, which are driven in the normal state. With an appropriate set of fitting parameters, both approaches fairly well describe current-voltage characteristics of the hot-electron mixer and predict reasonable values of the noise temperature and conversion efficiency. These models suggest that the noise temperature of the mixer, when corrected for optical losses, should not depend on the LO frequency unless it approaches the quantum limited value $h\nu/k_B$. On the contrary, analysis of the experimental data in the LO frequency range from 0.7 THz to 5.2 THz shows [6,8] that the DSB system noise temperature of the lattice-cooled hot-electron NbN mixer increases with frequency and that this increase can-not fully account for the optical losses. In this section we compare the performance of the same mixer optimally operated at LO frequencies 2.5 THz and 0.7 THz (118.8 μm and 432.6 μm) using the setup described earlier in this paper. Thorough analysis of the experimental data shows that there are more features in contradiction with the traditional model.

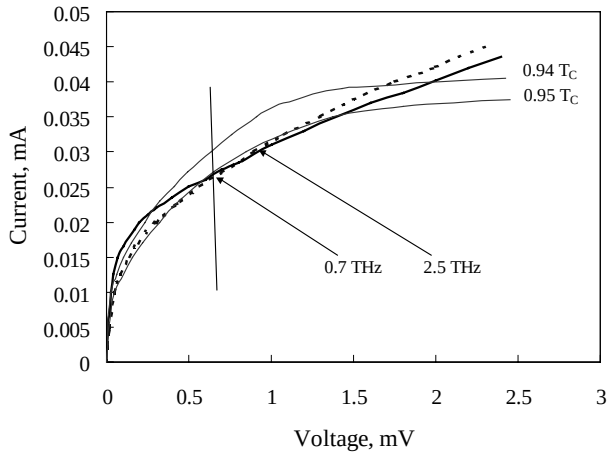

Fig. 4: CVC of the mixer with optimal LO power at 2.5 THz (dotted line) and 0.7 THz (thick solid line) recorded at the bath temperature 4.5 K and CVC without LO power (thin solid lines) recorded at 8.0 K (0.94 T_C) and at 8.1 K (0.95 T_C). Arrows point optimal bias regimes. The tilted straight line represents the trajectory of the operation point when the LO power changes.

Current-voltage characteristics (CVC) of the mixer are presented in Fig. 4. One can clearly see that optimal operation regimes for 2.5 THz and 0.7 THz are different and so are the CVC recorded with optimal LO power. It is worth noting that the ac resistance does not change much, thus providing in both regimes approximately the same matching of the device to the IF network. Characteristics recorded at an elevated temperature without local oscillator differ in shape from characteristics recorded at optimal LO power, although the temperature in the former case was adjusted in order to provide the best possible match between the two types of characteristic. Moreover, the noise power under optimal operation is noticeably larger when the mixer is pumped by the LO with smaller frequency. The corrected system noise temperature at 2.5 THz amounts 1140 K that is 1.6 times the corrected noise temperature at 0.7 THz, whereas the noise of the HEB drops almost twice within the same frequency interval. This observation implies that the mixer conversion efficiency decreases from -10 dB at 0.7 THz to -14.5 dB at 2.5 THz. The frequency dependence of the conversion efficiency may arise from the intrinsic mixing mechanism as well as from the frequency dependent coupling of radiation. We first consider the mixing mechanism.

A) Intrinsic Mixing Mechanism

Since the thermal approach relying on an elevated effective temperature of electrons and phonons does not suggest any frequency dependence we take into account effects inherent to the superconducting state. Indeed, it has been shown that suppression of superconductivity due to irradiation occurs differently depending on the energy of the radiation quantum $h\nu$, i.e. whether $h\nu$-2Δ (Δ is the energy gap) is small or large compared to the energy gap. Qualitatively, the high frequency limit corresponds to the steady-state nonequilibrium distribution function of quasiparticles, which are spread over the energy interval from Δ to $h\nu$. In the limiting case, $h\nu >> 2\Delta$, the temperature dependence of the energy gap under irradiation flattens compared to the equilibrium situation [14].

In the opposite limiting case, $h\nu - 2\Delta << 2\Delta$, quasiparticles are produced in the narrow energy interval above the gap. Detailed calculations of the nonequilibrium distribution function [15] show that, indeed, excess quasiparticles are located mostly around the energy $h\nu/2$ above the gap edge. The localized nonequilibrium distribution suppresses the energy gap in a manner similar to that suggested by the μ*-model [16]. In particular, this model predicts that under external pair breaking the gap initially decreases down to the value 0.62 Δ at which the first-order transition to the normal state occur. At small disturbances the first order transition is also expected for the energy gap versus temperature whereas under strong disturbance the slope of the transition becomes smoother and reaches the value typical for the transition in equilibrium. Thus, the rate of the gap decrease under external pair breaking should be larger at smaller radiation frequencies. In the mixing experiment, the difference between two limiting cases can be detected only if the resistance of the mixer in the operation point depends directly on the energy gap. We consider the superconducting strip with a normal domain. The bias current passing the interface between the domain and the remaining superconducting portion of the strip generates charge imbalance in the superconducting side. This is accompanied by penetration of the electric field into superconductor over the distance Λ_E. Each side of the domain contributes additional resistance $\rho\Lambda_E/S$ (ρ is the normal resistivity and S is the cross-section of the strip). The same additional resistance appears at each contact of the bolometer with normal metal. This simple picture strictly holds only if the penetration depth of the electric field is comparable or larger than the thermal healing length $\Lambda_T = (D\tau_\theta)^{1/2}$, which controls thermal smearing of the domain walls and, on the other hand, represents the smallest length of the normal domain. Here τ_θ and D are the electron cooling time and electron diffusivity, respectively. We estimate that for our NbN films in equilibrium at $T = 0.9\ T_C$ both thermal healing length and penetration length equal approximately 25 nm. Under optimal operation, the local oscillator suppresses the energy gap in the superconducting part of the bolometer. Though the exact value of the gap is hard to calculate, an estimate can be made comparing CVC (see Fig. 4) recorded with and without LO power. In our case the energy gap at optimal operation approximately equals the equilibrium energy gap at $T = 0.9\ T_C$. At optimal bias the dc resistance of the HEB ranges typically from 1/3 to 1/2 of the normal resistance that corresponds, for a 200-nm long device, to the normal portion of about 80-nm length. Thus, the charge imbalance may be responsible for the part of the resistance under optimal operation conditions. Both dr/dW and dr/dT, which mainly determine the conversion efficiency and the electric noise due to thermal fluctuations, bear contribution from the normal domain and from the charge imbalance regions. The contribution due to charge imbalance is determined by the actual value of the energy gap in the superconducting part of

the strip and, therefore, depends on the radiation frequency. The present qualitative model appears capable to explain why pumping of the mixer by the LO with larger frequency results in the decrease of the output noise. The model also suggests smaller conversion efficiency at higher LO frequencies due to the decrease of *dr/dW*. The mechanism described above does not necessarily result in variations of the system noise temperature with frequency since changes of the output noise power and conversion efficiency may compensate each other.

B) Coupling Efficiency

Dependence of the mixer performance on the LO frequency may arise due to the change of the coupling efficiency. We consider here coupling of the high frequency current flowing in the arms of the planar spiral antenna with the superconducting bolometer. The simplified, although, relevant prototype is an infinitely long slot line on a dielectric substrate and a metal strip which bridges opposite sides of the line to mimic the bolometer. Since the resistivity of the bolometer for the LO frequency is large compared to the resistivity of the contacts and its width is much smaller that the wavelength, one can use the quasi-static approximation to find the distribution of the current in the strip. Inside the strip, the electric field E of the frequency ω satisfies the equation [17].

$$\nabla^2 \vec{E} = i\frac{\omega \mu_0}{\rho}\vec{E} \qquad (1)$$

The thickness of the bolometer is small compared to the skin depth $\delta = (2\rho/\mu_0\omega)^{1/2}$, which in turn is much larger then the electron mean free path in NbN. We, therefore, deal with the normal skin effect and uniform distribution of the high frequency current through the film thickness. If the high frequency voltage U is fixed at the antenna terminals, the solution of Eq. 1 for the current distribution across the strip $j(x) = E(x)/\rho_n$ is given by

$$\begin{aligned} j(x) &= j_0\left(csh^2(x/\delta)\cos^2(x/\delta) + i\,sh^2(x/\delta)\sin^2(x/\delta)\right) \\ j_0 &= \frac{U}{\rho_n L}\left[csh(a/2\delta)\cos(a/2\delta) + i\,sh(a/2\delta)\sin(a/2\delta)\right]^{-1} \end{aligned} \qquad (2)$$

where x varies from –a/2 to a/2 and L is the bolometer length. Fig. 5 shows the distribution of the dissipated power $U(j(x)j^*(x))^{1/2}$ according to Equation 2 for frequencies 2.5 THz and 0.7 THz in a 1.7 μm wide strip having the normal resistivity 3.5 μΩ·m that is typical for our devices. One can see that at 2.5 THz power is absorbed mostly near the bridge edges. The central part of the strip remains in a regime, which is not optimal and effectively shunts the peripheral area of the device. The non-uniformity should result in the conversion efficiency smaller than it could be in the case of the uniform distribution of the high frequency current. Thus, hampering of the conversion efficiency due to non-uniformity should strengthen for our devices with frequency in the relevant frequency interval. Knowing the distribution of the current, it is straightforward to calculate the effective impedance of the strip and the coupling between the antenna and the mixer. For the equivalent circuit comprising the bolometer with the normal square resistance R_s and the antenna with the real impedance R_a, the radiation coupling efficiency is given by

$$K = \frac{4\dfrac{R_a}{R_s}\dfrac{2\delta}{L}\dfrac{sh(a/2\delta)+\sin(a/2\delta)}{csh(a/2\delta)-\cos(a/2\delta)}}{\left(\dfrac{sh(a/2\delta)-\sin(a/2\delta)}{csh(a/2\delta)-\cos(a/2\delta)}\right)^2+\left(\dfrac{sh(a/2\delta)+\sin(a/2\delta)}{csh(a/2\delta)-\cos(a/2\delta)}+\dfrac{R_a}{R_s}\dfrac{2\delta}{L}\right)^2} \qquad (3)$$

Due to the non-uniform distribution of the high frequency current, the conversion efficiency of the mixer should have approximately the same frequency dependence. We, therefore, compare the frequency dependence of the noise temperature with K^2 that accounts for both frequency dependent contributions. For calculations we used the antenna impedance 25 Ω, the normal square resistance 900 Ω and actual parameters of our device. Results of simulation are presented in Fig. 1. There is reasonable agreement between model results and experimental data at frequencies up to 4 THz. In this frequency range, decrease of the conversion efficiency with LO frequency explains almost uniquely the degradation of the mixer noise temperature. At higher frequency, displacement currents, which we did not take into account, may cause additional decrease of the coupling efficiency. Contribution to the frequency conversion that arises from the charge imbalance area may also modify the frequency dependence of the noise temperature. We believe that the frequency dependent non-uniform distribution of the high frequency current and the frequency dependent excess noise due to charge imbalance are both responsible for the increasing noise temperature of the HEB mixer at terahertz frequencies.

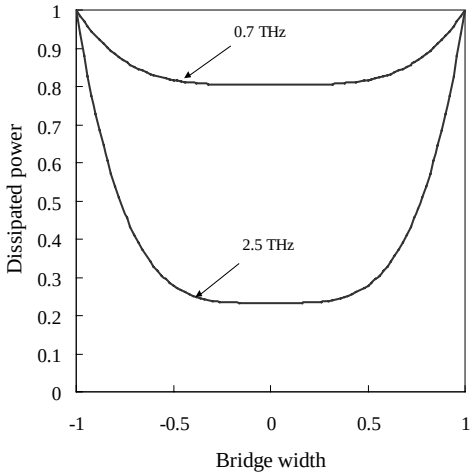

Fig. 5: Distribution of the dissipated high frequency power in the HEB. Position across the bolometer is plotted in units of its half width. The absorbed power is normalized to unity at the bolometer edges.

VI. CONCLUSION

We have shown that the noise temperature of the lattice-cooled hot-electron bolometer mixer increases with frequency and that this increase can not be explained neither by the frequency dependent parameters of the coupling optics nor by the conventional models of the hot-electron bolometer. We have developed a new model, which takes into account the non-uniform distribution of the high frequency current in the bolometer and the frequency dependent contribution to the electric noise and conversion efficiency steaming from charge imbalance phenomenon. We have demonstrated that the former effect explains almost by itself

the frequency dependence of the corrected noise temperature and the magnitude of the conversion losses in the frequency range from 0.7 THz to 4 THz. Further improvement of the performance of the HEB mixer may be achieved making use of narrower bolometers. This should result in more uniform current distribution and, consequently, in better coupling. To maintain the resistance of the bolometer and, thus, the maximal coupling efficiency unchanged, the length of the bolometer should be proportionally decreased. In addition, we have shown that Parylene works as an antireflection coating for Silicon at terahertz frequencies. An improvement of the noise temperature of about 30% at 2.5 THz was achieved by using a Silicon lens with a Parylene coating.

The work was supported by the German Ministry of Science and Education (WTZ RUS-149-97) and NATO Division of Scientific Affairs.

REFERENCES

[1] H. P. Röser, H.-W. Hübers, T. W. Crowe, W. C. B. Peatman, Infrared Phys. Technol. **35**, 451 (1994).

[2] A. L. Betz, R. T. Boreiko, Proc. of the 7th Int. Symp. on Space Terahertz Technology, 503 (1996).

[3] S. Cherednichenko, P Yagoubov, K. Il'in, G. Gol'tsman, E. Gershenzon, Proc. of the 8th Int. Symp. on Space Terahertz Technology, 245 (1997).

[4] S. Svechnikov, A. Verevkin, B. Voronov, E. Menschikov, E. Gershenzon, G. Gol'tsman, Proc. of the 9th Int. Symp. on Space Terahertz Technology, 45 (1998).

[5] J. D. Kraus, *Antennas*, McGraw-Hill, Inc., (1988).

[6] J. Schubert, A. Semenov, G. Gol'tsman, H.-W. Hübers, G. Schwaab, B. Voronov, E. Gershenzon, Supercond. Sci.Technology **12**, 748 (1999).

[7] H. Büttgenbach, R. E. Miller, M. J. Wengler, D. M. Watson, T. G. Phillips, IEEE Trans. on Microwave Theory Tech. **36**, 1720 (1988).

[8] H.-W. Hübers, J. Schubert, A. Semenov, G. Gol'tsman, B. Voronov, G. Gershenzon A. Krabbe, H. P. Röser, to appear in: Proc. of SPIE Conf. on Airborne Astronomy Systems, Munich, March 2000.

[9] D. Grischkowsky, S. Keiding, M. van Exter, Ch. Fattinger, J. Opt. Soc. Am. B **7**, 2006 (1990).

[10] P. G. J. Irwin, P. A. R. Ade, S. B. Calcutt, F. W. Taylor, J. S. Seeley, R. Hunnemann, L. Walton, Infrared Phys. **34**, 549 (1993).

[11] S. Nebosis,, A.D. Semenov, Yu.P. Gousev, and K.F. Renk, Proc. of the 7th Int. Symp. on Space Terahertz Technology, 601 (1996).

[12] D.Wilms Floet, E. Miedema, J.J.A. Baselmans, T.M. Klapwijk, J.R. Gao, IEEE Transactions on Applied Suprconductivity **9**, 3749 (1999).

[13] H. Merkel, P. Khosropanah, P. Yagoubov, E. Kollberg, IEEE Transactions on Applied Superconductivity **9**, 4201 (1999).

[14] V.F. Elesin, Sov. Phys. JETP **44**, 780 (1976).

[15] V.F. Elesin, Yu.V. Kopaev, Sov. Phys. Uspekhi (USA) **24**, 116 (1981).

[16] C.S. Owen and D.J. Scalapino, Phys. Rev. Lett. **28**, 1559 (1972).

[20] Landau and E.M. Lifshitz, Course of Theoretical Physics, vol. 8 (Electrodynamics of Continuous Media), Reed Educational and Professional Publishing Ltd, 1984, ISBN 0-750-62634-8.